Imidazol-1-ylethylindazole Voltage-Gated Sodium Channel Ligands Are Neuroprotective during Optic Neuritis in a Mouse Model of Multiple Sclerosis

Lorcan Browne,[†] Katie Lidster,[‡] Sarah Al-Izki,[‡] Lisa Clutterbuck,[†] Cristina Posada,[†] A. W. Edith Chan,[†] Dieter Riddall,[†] John Garthwaite,[†] David Baker,[‡] and David L. Selwood*,[†]

[†]Biological and Medicinal Chemistry, Wolfson Institute for Biomedical Science, University College London, Gower Street, London WC1E 6BT, United Kingdom

[‡]Neuroimmunology, Blizard Institute, Barts and the London School of Medicine and Dentistry, Queen Mary University of London, 4 Newark Street, London E1 2AT, United Kingdom

Ⓢ *Supporting Information*

ABSTRACT: A series of imidazol-1-ylethylindazole sodium channel ligands were developed and optimized for sodium channel inhibition and in vitro neuroprotective activity. The molecules exhibited displacement of a radiolabeled sodium channel ligand and selectivity for blockade of the inactivated state of cloned neuronal Na_v channels. Metabolically stable analogue **6** was able to protect retinal ganglion cells during optic neuritis in a mouse model of multiple sclerosis.

Na_v activity
Non-immunosuppressive

Neuroprotective in optic neuritis - Multiple Sclerosis model
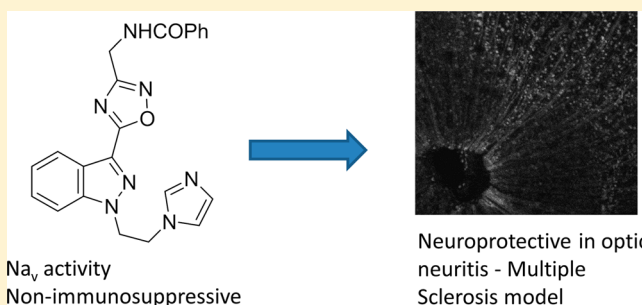
INTRODUCTION

Voltage-gated sodium (Na_v) channels are the fundamental generators of electrical impulses (action potentials) in the membranes of excitable cells. A number of clinically used drugs exert their therapeutic effects through Na_v. These drugs are primarily used in the treatment of central nervous system (CNS) disorders, such as epilepsy and neuropathic pain, but are increasingly being scrutinized as potential treatments for neurodegenerative conditions occurring acutely, such as in ischemic stroke, or chronically, as in multiple sclerosis (MS).[1] Phenytoin **1** was one of the first antiepileptics developed (Figure 1). It exerts a voltage-dependent and frequency-dependent block of Na^+ currents. This selectivity is suggested to be the reason for its lack of significant cognitive side effects.[2] Other first-generation antiepileptics that act on Na_v channels include lamotrigine **2**,[3] and carbamazepine **3**[4] (Figure 1). Recently, lacosamide **4** was approved for use in partial-onset seizures and neuropathic pain. Lacosamide is proposed to act via an unique mechanism of state-dependent blockade of Na_v channels: stabilizing channels in a slow inactivated state without effects on fast inactivation.[5]

Nine Na_v channel isoforms have been identified, of which, Na_v1.1, 1.2, 1.3, and 1.6 are predominately found within the CNS, whereas Na_v1.7, 1.8, and 1.9 are located in the peripheral nervous system. Na_v1.4 is found within skeletal muscle, and Na_v1.5 is found in the heart. The Na_v isoforms are also expressed outside their primary tissues.[6] Recently, the first X-ray crystal structure of a voltage-gated sodium channel was solved: initially in the closed state and subsequently in two
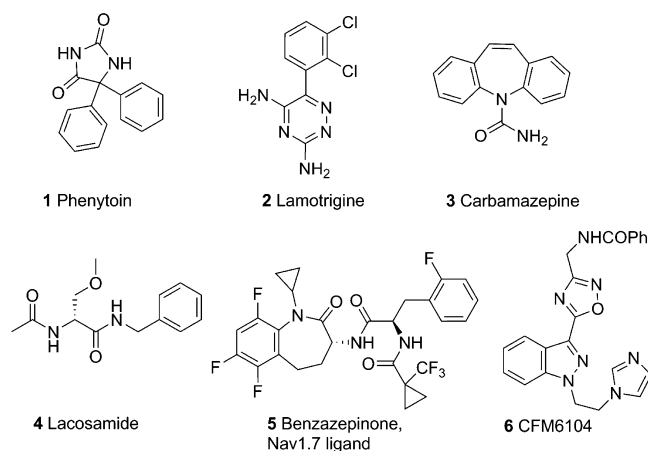

Figure 1. Compounds with sodium channel modulatory activity.

presumed inactivated states.[7,8] Under normal physiological conditions, the channels interconvert between different functional states: the resting state in which the channel pore is closed, an open state in which the channel pore is open and permeable to Na^+, and one or more inactivation states where the pore is open but blocked.[9]

Recent studies have highlighted the importance of Na_v1.3, 1.7, 1.8, and 1.9 in various pain syndromes.[10−12] Notably,

Scheme 1[a]

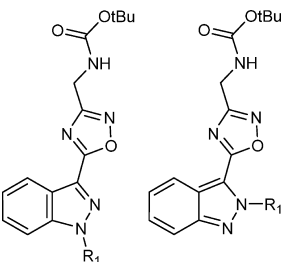R$_1$ = alkylheterocycles
R$_2$ = ArSO$_2$ or ArCO
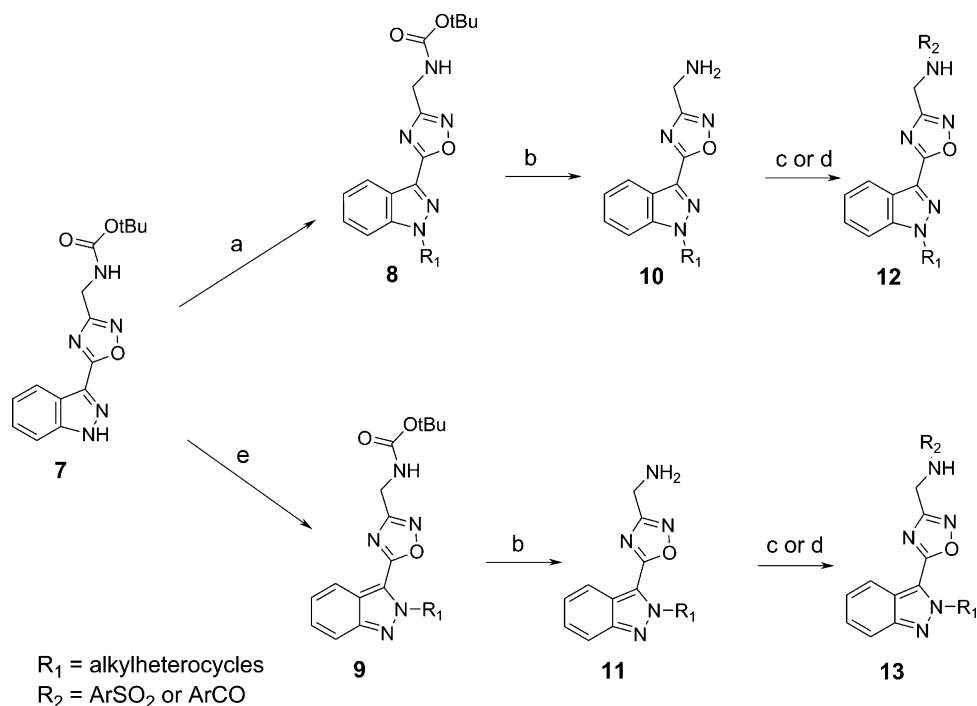
[a](a) R$_1$-bromide/chloride, Cs$_2$CO$_3$, DMF; (b) TFA, TIPS, H$_2$O, (c) ArCOOH, 2-(7-aza-1H-benzotriazole-1-yl)-1,1,3,3-tetramethyluroniumhexa-fluorophosphate (HATU); (d) ArSO$_2$Cl, Na$_2$CO$_3$; (e) R$_1$-alcohol, tributylphosphine, TMAD, PhMe.

genetically inherited pain disorders have been associated with mutation of these Na$_v$ encoding genes.[13] Clinically, carbamazepine, lamotrigine, and phenytoin are all used to treat neuropathic pain.[14] The Merck, Pfizer, AstraZeneca, and GlaxoSmithKline pharmaceutical groups have all independently reported their own series of 1.3-, 1.7-, and 1.9-selective sodium channel modulators for use in neuropathic pain,[15] exemplified here by the benzazepinone compounds from Merck Pharmaceuticals, such as 5 (Figure 1).[16,17]

Sodium channel blockers can exhibit significant neuroprotective effects.[18] Influx of sodium from the extracellular space during reperfusion plays a major role in excitotoxic neuronal death after cerebral ischemia.[19] Block of Na$_v$ channels can attenuate the primary events that occur in an ischemic attack, most likely by blocking Na$^+$ permeability, resulting in reduced ATP depletion and reduced ischemic-induced release of glutamate.[20] A number of drugs, including lamotrigine, BW-1003C87, the local anesthetic lidocaine, and sipatrigine, have all shown neuroprotective effects in animal models of stroke.[21−24] However, as of yet, these results have failed to translate into beneficial effects in clinical trials.[25,26] Thus, there is a need for drugs with a better clinical efficacy and therapeutic index. Treatment of stroke is limited by the fact that administration of treatment in humans only occurs sometime after the onset of the neurodegenerative insult. In contrast, for slowly evolving neurodegenerative conditions, it is possible to treat during or even before individual neurodegenerative episodes occur. Carbamazepine (3) is commonly used to alleviate the symptoms of MS, such as spasms, nerve pain, and trigeminal neuralgia, and lamotrigine has been trialled in neuroprotection.[27] Research into the potential neuroprotective effects of these compounds is gaining increasing momentum because of a better understanding of the role of Na$_v$ channels in nerve damage.[28]

To understand the role of individual Na$_v$ channel isoforms in neuroprotection, we need to consider their distribution. Although most of the sodium channel variants are expressed at different levels in the CNS, Na$_v$1.6 expression is widespread[29] but is more abundant in nerves of the retina, cerebellum, and cortex tissue.[30] In a mature, myelinated axon, Na$_v$1.6 tends to cluster and is the predominant isoform at the nodes of Ranvier.[31] A significant increase in Na$_v$1.6 density can be seen subsequent to nerve fiber injury in traumatic brain injury and multiple sclerosis.[32−34] Na$_v$1.6 has also been implicated in secondary degeneration of neuronal cells. Mechanical, ischemic, and inflammatory insult can, over time, contribute to this degeneration. Shear and stretch forces, despite not destroying the cells or severing the axons can, nonetheless, produce secondary degeneration in brain tissues.[35] Rapid tetrodotoxin-sensitive calcium overload occurs in stretch-traumatized axons, which suggests that in neuropathologic conditions structural degradation of the axolemmal bilayer can foster a chronically left-shifted Na$_v$ channel operation. This points to leaky Na$_v$ channels playing an important role in determining neuronal cell survival.[36] Other Na$_v$ channel isoforms, namely, Na$_v$1.1[37] and Na$_v$1.3, have also been implicated in traumatic brain injury models.[38] Overall, there is no clear understanding of the specific contributions of each isoform to the neuroprotective effect; we anticipate that investigations of the action of well-characterized compounds will aid in this regard. Previous work by this group designed a class of voltage-dependent sodium channel modulators based on the indazolyloxadiazolyl scaffold.[39] Further development of analogues around this scaffold has now identified a series of imidazolylethylindazoles with good neuroprotective effects. Following assessment of sodium channel isoform selectivity and functional activity, a candidate molecule, CFM6104, 6 (Figure 1), was tested in an in vivo optic neuritis (inflammation of the optic nerve) mouse model

Table 1. Sodium Channel Modulatory and Neuroprotective Activity of Boc-Protected Oxadiazolyindazole Analogues

compound	R (isomer)	[^{3}H]sipatrigine binding, IC$_{50}$ (μM)	neuroprotection at 50 μM (%)
lamotrigine		1.8 ± 0.2^a	33^b
tetrodotoxin			100^c
sipatrigine		0.04 ± 0.001^a	93^d
14	CH$_2$-Ph (N$_1$)	8.3^e	19^e
15	CH$_2$-Ph (N$_2$)	5.5^e	25^e
16	CH$_2$CH$_2$-2-imidazole (N$_1$)	7.4 ± 1.1	56 ± 5.6 (4)
17	CH$_2$CH$_2$-2-imidazole (N$_2$)	15.5 ± 9.2	35 ± 5.3 (3)
18	2-py (N$_1$)	74 ± 20.4	18 ± 7.1 (4)
19	CH$_2$-2-py (N$_2$)	23 ± 5.9	42 ± 3.8 (4)
20	CH$_2$CH$_2$-2-thiophene (N$_2$)	166 ± 49	1 ± 13.4 (4)
21	CH$_2$-4-(5-CH$_3$)-isoxazole (N$_1$)	339 ± 121	39 ± 7.8 (4)
22	CH$_2$-C$_6$H$_4$-N-pyrazole (N$_1$)	617 ± 160	20 ± 16.4 (3)
23	CH$_2$-3,4-benzodioxole (N$_1$)	6 ± 1.0	−3 ± 6.2 (4)

^{a}Values reported in literature.[39] ^{b}Tested at 30 μM. Results are normalized to the effect of TTX and are based on the mean of at least three experiments. ^{c}TTX tested at 1 μM. ^{d}Tested at 3 μM. ^{e}Reported previously.[39]

of MS and found to prevent the consequent loss of retinal nerve cells.

RESULTS

Design. In our previous investigations, we demonstrated that aminomethyloxadiazolylindazoles had good neuroprotective activity. If the amino group was protected as a Boc group, then the activity was generally lost. However, exploration of alternative groups to the indazole N$_1$/N$_2$ benzyl revealed a Boc-protected intermediate (vide infra) with surprising neuroprotective activity. This molecule exhibited a different SAR profile to the previous series with lower cytochrome P450 inhibition. We therefore carried out a detailed investigation of the neuroprotective activities of this series. Key objectives were to maintain the neuroprotective activity and to improve the metabolic stability to allow evaluation in vivo.
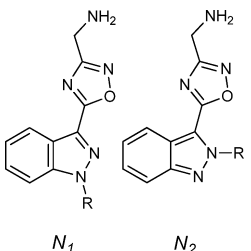
Chemistry. The synthesis of 3-[3-*tert*-butoxycarbonylaminomethyl-1,2,4-oxadiazol-5-yl]indazole 7 (Scheme 1) has been previously described.[39] This compound was utilized as a key synthetic intermediate for the production of a further series of compounds. The stereoselective synthesis of alkyl N$_1$- and N$_2$-heteroaromatic-substituted compounds (Scheme 1) was carried out using a cesium- or potassium carbonate-mediated alkylation of an alkyl halide-functionalized heteroaromatic compound (N$_1$), 8, or a Mitsunobu reaction with an alcohol-functionalized heteroaromatic compound (N$_2$), 9. Boc removal was performed using trifluoroacetic acid, triisopropylsilane, and water to yield the free amines 10 and 11. These amines were then derivatized to provide the N$_1$ 12 and N$_2$ 13 analogues shown. The benzamides were formed via a coupling reaction between the free amine and R-substituted benzoic acid in the presence of DMF, HATU, and DIPEA at room temperature. This reaction occurred at various efficiencies (9−75%) across the range of substituted oxadiazolylindazoles and substituted benzoic acids. The sulfonamide analogues were formed by reaction of the free

amine with R-substituted benzene sulfonyl chloride in the presence of sodium carbonate at room temperature with reaction efficiencies of 24−39%.

Biological Assays. Activity against sodium channels was assessed using a radioligand binding assay using [^{3}H]sipatrigine as the ligand[39] and by patch-clamp electrophysiology on cloned human channels. The in vitro neuroprotection assay was an adaptation of an original study by Fowler and Li.[40] In this system, rat hippocampal slices are subjected to oxygen-glucose deprivation, and the subsequent progression to cell death is monitored by determining their ATP levels. This paradigm is highly sensitive to blockade of sodium channels and tetrodotoxin. The compounds were also tested for metabolic stability in rat liver microsomes. Na$_v$ channel isoform activity was determined using an automated patch-clamp system against hNa$_v$1.1−hNa$_v$1.8/β3 expressing cells. T-cell immunosuppressive activity was assessed using a simple contact hypersensitivity model that detects T-cell proliferation to oxazolone in lymphnodes.[41−43] In vivo neuroprotection was evaluated in an optic neuritis model[44] using double-transgenic mice expressing both a Thy1-promoter-driven cyan fluorescent protein restricted to retinal ganglion cells and a myelin oligodendrocyte glycoprotein T-cell receptor (TCR).[44] Following injection of *Bordetella pertussis* toxin, the mice develop subneurological experimental autoimmune encephalomyelitis (EAE) and optic neuritis in the optic nerve, which then leads to retinal ganglion cell loss secondary to axon damage.

Activity against Sodium Channels and Neuroprotection. Initial testing with N$_1$- and N$_2$-functionalized *tert*-butyl carbamate-protected analogues showed encouraging results in the [^{3}H]sipatrigine binding and neuroprotection assays (Table 1). Lamotrigine, sipatrigine, and tetrodotoxin were included as reference molecules. Benzyl-functionalized molecules 14 and 15, reported in previous work, are shown for comparison.[39] A
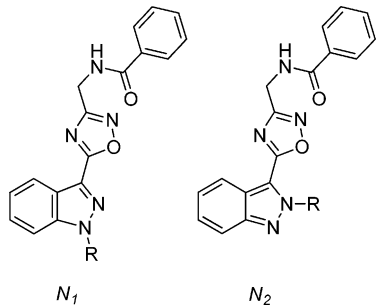
Table 2. Sodium Channel Modulatory and Neuroprotective Activity of Oxadiazolylindazole Analogues

compound	R (isomer)	[^{3}H]sipatrigine binding, IC$_{50}$ (μM)	neuroprotection at 50 μM (%)
lamotrigine		1.8 ± 0.2[a]	33[b]
tetrodotoxin			100[c]
sipatrigine		0.04 ± 0.001[a]	93[d]
24	CH$_2$-Ph (N$_1$)	3.3 ± 0.6[e]	>99,[e] **35 ± 9.0**
25	CH$_2$-Ph (N$_2$)	7 ± 2.8[e]	57 ± 15.6 (4)
26	CH$_2$CH$_2$-2-imidazole (N$_1$)	148 ± 120	−2 ± 1.9 (3)
27	CH$_2$CH$_2$-2-imidazole (N$_2$)	14 ± 1.6	8 ± 26.9 (4)
28	2-py (N$_1$)	32 ± 8.2	−11 ± 13.8 (4)
29	CH$_2$-2-py (N$_2$)	>10 000	25 ± 9.4 (4)
30	CH$_2$CH$_2$-2-thiophene (N$_2$)	0.6 ± 0.05	36 ± 5.4 (4)
31	CH$_2$-4-(5-CH$_3$)- Isoxazole (N$_1$)	15 ± 5.4	19 ± 8.6 (4)
32	CH$_2$-C$_6$H$_4$-N-pyrazole (N$_1$)	6.2 ± 3.8	26 ± 9.0 (4)
33	CH$_2$-3,4-benzodioxole (N$_1$)	2.1 ± 0.3	44 ± 2.8 (4)

[a]Values reported in literature.[39] [b]Tested at 30 μM. Results are normalized to the effect of TTX and are based on the mean of at least three experiments. [c]TTX tested at 1 μM. [d]Tested at 3 μM. [e]Reported previously[39] (values in bold are IC$_{50}$'s in micromolar).

Table 3. Sodium Channel Modulatory and Neuroprotective Activity of Benzamide-Functionalized Oxadiazolylindazole Analogues

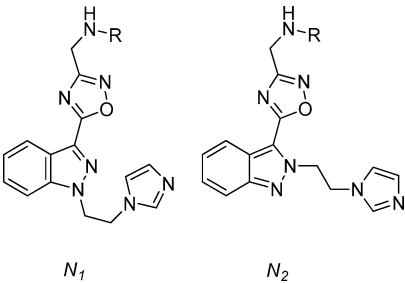| compound	R (isomer)	[^{3}H]sipatrigine binding, IC$_{50}$ (μM)	neuroprotection at 50 μM (%)
lamotrigine		1.8 ± 0.2[a]	33[b]
tetrodotoxin			100[c]
sipatrigine		0.04 ± 0.001[a]	93[d]
6	CH$_2$CH$_2$-N-imidazole (N$_1$)	13 ± 9	47 ± 15.1 (4)
34[e]	CH$_2$CH$_2$-N-imidazole (N$_2$)	4.5 ± 0.3	**19 ± 1.2**
			41 ± 9.4 (4)
35	CH$_2$-2-py (N$_2$)	41 ± 7	58 ± 4.6 (4)
36	CH$_2$CH$_2$-2-thiophene (N$_2$)	>1000	−2 ± 6.2 (4)
37	CH$_2$-4-(5-CH$_3$)-isoxazole (N$_1$)	>2000	19 ± 20.0 (4)

[a]Values reported in literature.[39] [b]Tested at 30 μM. Results are normalized to the effect of TTX and are based on the mean of at least four experiments. [c]TTX tested at 1 μM. [d]Tested at 3 μM. Values in bold are IC$_{50}$'s in micromolar. [e]Tested as a mixture of 83% N$_1$ and 17% N$_2$ isomers.

combination of reasonable potency (20 μM) and >30% neuroprotection identifies active compounds.

Replacement of the benzyl group with substituted and nonsubstituted heteroaromatic groups showed a general decrease in the ability of the compounds to displace the radioactive ligand, with the notable exceptions of the ethylimidazole analogues **16** and **17** (Table 1). Other side chains with weakly basic pyridyl moieties, **18** and **19**, demonstrated moderate binding and neuroprotective activity, whereas nonbasic heterocycles **20** and **21** or bulkier groups **22** and **23** displayed weak binding or low neuroprotection.

In the previous series, a free amine group led to a general increase in the neuroprotection by the benzylindazole analogues (e.g., compounds **24** and **25**; Table 2). That trend was not observed here. The modest neuroprotection observed for the imidazole and pyridine analogues was removed with free amines such as **26** and **27**. This was also the case for the pyridyl−free amines **28** and **29**. The neutral side chains

Table 4. Sodium Channel Modulatory and Neuroprotective Activity of N_1- and N_2-Propylimidazole-Functionalized Oxadiazolylindazole Analogues

N_1 N_2

compound	N_1/N_2 functionalized	R	[^{3}H]sipatrigine binding, IC$_{50}$ (μM)	neuroprotection at 50 μM (%) or EC$_{50}$ (bold)
lamotrigine			1.8 ± 0.2^a	33^b
tetrodotoxin				100^c
sipatrigine			0.04 ± 0.001^a	93^d
38	N_1	CO-2,3,4-(OCH$_3$)$_3$Ph	5.3 ± 2.8	37 ± 6.4 (4)
39	N_1	CO-4-indole	13 ± 2.0	52 ± 9.9 (4)
40	N_1	CO-4-t-BuPh	1.2 ± 0.2	40 ± 34.2 (4)
41	N_1	CO-2,3-(OCH$_3$)$_2$Ph	7.1 ± 0.8	69 ± 7.5 (4)
42	N_1	CO-3-OCF$_3$Ph	1.5 ± 0.3	37 ± 13.0 (4)
43	N_2	CO-4-ClPh	2.2 ± 0.5	42 ± 3.1 (4)
44	N_2	CO-2,3-F$_2$Ph	3.6 ± 0.2	2 ± 1.4 (4)
45	N_2	CO-4-OCF$_3$Ph	0.7 ± 0.1	31 ± 8.2 (4)
46	N_2	CO-2-CH$_3$Ph	2.9 ± 0.5	62 ± 4.4 (4)
47	N_2	CO-4-OCH$_3$Ph	6.2 ± 0.7	55 ± 10.7 (4)
48	N_2	CO-4-(NHCOCH$_3$)Ph	59 ± 31	-14 ± 3.6 (4)
49	N_2	CO-2-naphthalene	0.4 ± 0.2	22 ± 4.4 (4)
50	N_2	CO-2,3-(OCH$_3$)$_2$Ph	5.8 ± 1.8	**12.3 ± 5.8** 88 ± 7.7 (4)
51	N_2	CO-3-OCF$_3$Ph	0.6 ± 0.1	**5.15 ± 0.15** 78 ± 4.2 (4)
52	N_2	CO-(3-CH$_3$-4-NO$_2$)Ph	1.7 ± 0.2	43 ± 3.1 (4)
53	N_2	CO-3,4-benzodioxole	5.0 ± 0.4	27 ± 4.5 (3)
54	N_2	CO-3-CH$_3$Ph	2.5 ± 0.2	41 ± 6.9 (3)
55	N_2	CO-2-OCH$_3$Ph	7.1 ± 1.2	54 ± 11.3 (4)
56	N_2	CO-3-OCH$_3$Ph	5.0 ± 1.1	63 ± 7.6 (4)
57	N_1	SO$_2$-4-ClPh	10 ± 7.1	21 ± 7.9 (4)
58	N_1	SO$_2$-2,3-(OCH$_3$)$_2$Ph	>500	37 ± 2.5 (4)
59	N_1	SO$_2$-4-OCF$_3$Ph	4.9 ± 6.0	0 ± 9.9 (4)
60	N_1	SO$_2$-2-CH$_3$Ph	4.9 ± 1.3	57 ± 10.8 (4)
61	N_1	SO$_2$-3-CF$_3$Ph	2.1 ± 0.6	38 ± 12.3 (4)
62	N_1	SO$_2$-4-t-BuPh	4.4 ± 1.3	16 ± 20.2 (4)
63	N_2	SO$_2$-Ph	1.7 ± 0.5	**29.5 ± 3.8** 38 ± 14 (4)
64	N_2	SO$_2$-4-(NHCOCH$_3$)Ph	17 ± 6.8	25 ± 15 (4)

^{a}Values reported in literature.[39] ^{b}Tested at 30 μM. Results are normalized to the effect of TTX and are based on the mean of at least three experiments. ^{c}TTX tested at 1 μM. ^{d}Tested at 3 μM (values in bold are IC$_{50}$'s in micromolar).

ethylthiophene **30**, methylisoxazole **31**, and substituted benzyls **32** and **33** all showed good binding and modest neuroprotection.

These results supported the idea that the activity observed for the indazoles substituted by basic heterocycles at the N_1 position was not following a similar SAR pattern to the original series and required a lipophilic group at the oxadiazolylmethyl-amine. When the free amine analogues were functionalized with a benzamide group at the amine moiety, the neuroprotection and the radioligand-displacement ability of some of the analogues was improved, with moderate to good levels of binding observed for N_1 and N_2 imidazole analogues **6** and **34** (Table 3). Thus, it appeared that a benzamide group could

mimic the action of the *tert*-butyl carbamate. Methylpyridyl analogue **35** showed modest binding, whereas ethylthiophene **36** and methyloxazole **37** were essentially inactive.

On the basis of these encouraging effects, a new set of N_1 and N_2 imidazole analogues was designed and synthesized to see if improved binding and neuroprotective activity was achievable. The new set of N_1 and N_2 ethyl-2-imidazoles (compounds **38**–**64**, Table 4) showed a range of activity, with most showing good ability to displace the radioligand [^{3}H]sipatrigine, and a range of neuroprotective activity, many with moderate to good neuroprotection. In the N_1-substituted series, all but one of the 11 new analogues had a binding IC$_{50}$ < 13 μM, with some compounds having values as low as 1 μM. Similarly, in the N_2-

substituted series, all but one of the 16 new analogues had a binding IC_{50} < 17 μM, with some as low as 0.4 μM. Neuroprotection efficacy also showed a general increase, with compound **50** reaching 88% neuroprotection. In the N_1 series, the most profound effect was the 2,3-dimethoxy substitution of the benzamide ring, **41**, which led to a marked increase in displacement ability (IC_{50} 13 to 7.1 μM) and neuroprotection (46 to 71%). Interestingly, the analogous trisubstitution at the 2,3,4-positions, **38**, resulted in a decrease in neuroprotection. These aside, in the N_1 series, functionalization the benzamide changed little in terms of activity from the parent, **6** (IC_{50} range of 1−13 μM and neuroprotection range of 37−52%), with the potential to add larger groups, such as a indole **39** or *t*-butyl **40**, without significant loss of binding or neuroprotection. Compared to the N_1 series, the N_2 benzamide series had a much greater range of activities, both in binding (0.4−59 μM) and neuroprotection (2−89%). The 2-, 3-, and 4-methoxybenzamides all showed good binding (IC_{50} < 8 μM) and neuroprotection (54−63%), with the 2,3-dimethoxy-substituted benzamide once again showing the best activity with good binding (IC_{50} = 5 μM) and excellent neuroprotection (89%, EC_{50} = 12.3 ± 5.8). The benzamide substituted at the 3 position with OCF_3 showed comparable activity with binding (IC_{50} = 0.8 μM) and neuroprotection (80%). The only other marked effect was an almost total ablation of neuroprotective effect by fluorination at the 2 and 3 positions, despite showing an IC_{50} of 4 μM in the radioligand-displacement assay. Of all of the sulfonamide compounds in the N_1 series, only one improved on the neuroprotection of parent benzamide **6**, although many showed better binding. The 2- and 3-substituted sulfonamide showed good binding and modest neuroprotection, but substitution at the 4 position seemed to provide compounds with poor neuroprotective ability, if not binding, such as **57**, **59**, and **62**. In the N_2 series, the sulfonamide analogue of **34**, **63**, showed comparable binding and neuroprotection, but once again, a 4-substituted sulfonamide, **64**, had poorer binding and reduced neuroprotection. In fact, 4-substituted sulfonamide and benzamide analogues across the group had reduced capacity for neuroprotection in the hippocampal slice assay when compared to the 2- or 3-substituted or unsubstituted compounds, despite no significant difference in binding. The presence of unfavorable interactions at the 4 positions is indicated, and this may also account for the observation that small substituents such as Cl have a lesser detrimental effect on activity than larger groups. In the limited number of halide-functionalized benzamides and sulfonamides tested, none showed improved neuroprotection.

Stability in Rat Liver Microsomes. The N_1 and N_2 ethyl-2-imidazole-substituted series was examined for metabolic stability in rat liver microsomes. Table 5 shows a select subset of the compounds screened for rate of turnover. When examined, 14 of 21 compounds tested in this series had turnovers of greater than 90% after 40 min. Boc-protected and free amine N_2 analogues **17** and **27** showed better metabolic resistance, with turnovers of 70 and 57 min, respectively. Functionalization of the amine with benzamide, **34**, again produced an unstable compound. However the N_1 analogue, **6**, showed better stability with more than half of the original compound left after 40 min. Despite this promising result, none of the further analogues managed to maintain or improve on this stability, with any substitution making the compounds significantly more labile to metabolic degradation (>90%). Five benzamide and sulphonamide analogues that were fluorine- or

Table 5. Metabolic Stability Measured in a Rat Liver Microsome Assay for N_1- and N_2-Propylimidazole-Functionalized Oxadiazolylindazole Analogues

compound	turnover at 40 min (%)
17	70
27	57
34	97
6	47
42	78
63	97
64	54
48	45

chlorine-substituted at the 4, 5, and 6 positions on the indazole ring were also tested to see if this modification could arrest the rate of metabolism. All showed >90% metabolism after 40 min (data not shown). The only compound with moderately increased stability was the CO-3-OCF_3Ph-substituted benzamide, **42**. Similarly, substitution of the benzamide or changing to a sulfonamide did not provide much improvement in the metabolic stability of the N_2 analogues of benzamide **34**. Interestingly, however, substitution at the 4 position with the amide group, $NHCOCH_3$, in both the sulfonamide **64** and benzamide **34** analogues gave significant improvement in stability, with turnovers of 54 and 45%, respectively, after 40 min. Unfortunately, these 4 position-substituted $NHCOCH_3$ compounds were also some of the most inactive compounds in the neuroprotective assay.

Na_v Channel Isoform Profiling. Compounds **6** and **51** were examined by patch-clamp electrophysiology to determine their effects on sodium channel isoforms (Table 6 and Figure 2). Compound **6** showed preferential activity for the inactivated state (Figure 2A) but little discrimination between subtypes. The block of Na_v1.1, 1.3, and 1.6 is implicated in the pharmacological basis of neuroprotection (vide supra), and activity was noted against these isoforms consistent with the compounds' ability to displace radiolabeled sipatrigine (Table 6). Compound **51** showed good activity in both the radioligand-displacement and neuroprotection assays, and this is reflected in its potent block across the range of isoforms. It blocks many of the isoforms at an order of magnitude lower concentration than **6**, with its most potent block against the Na_v1.5 sodium channel, an isoform found primarily in cardiac muscle. There also appears to be less functional selectivity compared to **6** (Figure 2B). The potency of **51** against Na_v1.1, 1.3, and 1.6 when compared to **6** may account for the observed increase in neuroprotection seen with this compound (Table 6).

In Vivo Activity in an Optic Neuritis Mouse Model of MS. Compound **6** was selected for detailed in vivo evaluation on the basis of its mix of properties: in vitro sodium channel activity, activity against the neuronal Na_v isoforms, functional selectivity, and stability in rat liver microsomes. The influence of **6** was assessed in vivo in wild-type and myelin oligodendrocyte glycoprotein-specific T-cell receptor transgenic mice (Figure 4; 5).[44] First, **6** was examined for T-cell immunosuppressive activity, as the EAE model of MS is well-known to be T-cell-dependent.[45] Rather than use transgenic mice where all T-cells have the same specificity, a contact-hypersensitivity model was used because it is known to be predictive in identifying in vivo immunosuppressive doses for EAE studies.[41−43] Doses of **6** ranging from 5−50 mg/kg were

Table 6. Summary of Action of Compounds 6 and 51 on Na$_v$1.1−1.8

compound	tonic block (a)		10 Hz block (b)		inactivated-state block (c)		IC$_{50}$ b/c[b]	IC$_{50}$ a/c
	IC$_{50}$	n^a	IC$_{50}$	n	IC$_{50}$	n		
				Na$_v$1.1				
6	>100		>100		21 ± 6.29	1.71 ± 0.73	>5	>5
51	15.3 ± 5.02	1.09 ± 0.24	8.54 ± 0.72	1.32 ± 0.16	2.55 ± 0.22	2.09 ± 0.32	3.3	6
				Na$_v$1.2				
6	71 ± 25	1.12 ± 0.51	46 ± 7.42	1.82 ± 0.73	29 ± 1.49	1.48 ± 0.38	1.6	2.4
51	65 ± 22	0.48 ± 0.14	24.1 ± 3.87	0.63 ± 0.14	3.54 ± 1.24	0.6 ± 0.12	6.8	18
				Na$_v$1.3				
6	>100		>100		22 ± 4.09	0.78 ± 0.15	>5	>5
51	>100		97 ± 72	0.35 ± 0.19	4.76 ± 0.92	0.96 ± 0.19	20	>25
				Na$_v$1.4				
6	>100		56 ± 16.4	1.21 ± 0.36	24 ± 2.98	1.43 ± 0.27	2.3	>5
51	18.3 ± 1.65	1.23 ± 0.18	10.5 ± 0.47	1.34 ± 0.13	4.58 ± 0.25	1.75 ± 0.12	2.3	4
				Na$_v$1.5				
6	>100		69 ± 31	1.16 ± 0.54	19 ± 3.06	0.99 ± 0.22	3.6	>5
51	36 ± 19	0.76 ± 0.23	14.8 ± 7.52	0.37 ± 0.13	0.92 ± 0.89	0.49 ± 0.15	16	39
				Na$_v$1.6				
6	>100		>100		24 ± 7.3	2.45 ± 2.59	>5	>5
51	>100		32.2 ± 25.9	0.42 ± 0.19	3.32 ± 0.53	1.17 ± 0.18	9.7	>30
				Na$_v$1.7				
6	37 ± 7.0	2.09 ± 1.73	28 ± 1.8	1.88 ± 0.53	14.5 ± 0.73	2.24 ± 0.17	1.9	2.6
51	5.64 ± 0.57	2.59 ± 0.41	4.82 ± 0.33	2.63 ± 0.33	3.02 ± 0.36	2.5 ± 0.1	1.6	1.9
				Na$_v$1.8				
6	>100		>100		28 ± 0.97	1.42 ± 0.1	>4	>4
51	6.34 ± 1.08	2.14 ± 0.51	5.66 ± 1.47	2.62 ± 1.05	3.77 ± 0.49	2.75 ± 0.66	1.5	1.7

[a]n = the slope of the fit. [b]The ratio of IC$_{50}$ a/c and b/c illustrates the degree of functional selectivity for the inactivated state.

administered intraperitoneally (i.p.) from day −1 to day 2, and the in vivo induced proliferative response was assessed in the draining lymph nodes 3 days (the peak time of T-cell proliferation) after the sensitization to the contact-sensitizer oxazolone on day 0. There was no evidence suggestive of any inhibitory effect of sensitization based on cell numbers within the lymph nodes or based on a per cell proliferative response (Figure 3). Importantly, this study demonstrated that the drug was well-tolerated and there was no apparent toxicity. We next sought to assess whether **6** could exert a neuroprotective effect and limit the amount of axonal and nerve loss that results as a consequence of T-cell autoimmunity within the CNS. Following the development of optic neuritis in our model mice, demyelination was augmented following injection of 250 μg of Z12 rat IgG2b demyelinating antibody on day 14.[44] Retinal ganglion cell survival following treatment of animals with 5 mg/kg i.p. **6** was assessed on day 21 postinduction in retinal flatmounts (Figures 3A,B and 4). It was found that **6** increased ganglion cell survival ($P < 0.02$) and reduced the mean retinal loss from 914 ± 117 to 1298 ± 77 cells/mm^2 compared to 1653 ± 89 cells/mm^2 in a group of age-matched control animals without optic neuritis (Figure 4). This study suggests that this class of compounds may have some utility in controlling the accumulation of nerve loss that occurs in diseases such as MS.

■ DISCUSSION

During MS, Na$_v$ channels are redistributed along demyelinated nerves, which can help to restore function to some extent but leaves them vulnerable to excessive sodium entry.[18]

Our strategy was to develop compounds with good activity toward sodium channel inhibition, in particular against the neuronal isoforms Na$_v$1.1, 1.3, and 1.6, but, most importantly, which could also display neuroprotective capabilities in an in vitro hippocampal slice assay system. The selection of a candidate molecule for in vivo studies was based on a balanced assessment of properties, principally sodium channel activity, neuroprotection, and in vitro stability. The use of the hippocampal slice model, measuring ATP levels and tuned for sodium channel blockade, was key in ensuring an appropriate functional effect. In general, the series was found to exhibit poor stability in rat liver microsomes in vitro, with **6** being a notable exception that allowed us to test this paradigm in vivo. There are reports on the metabolism of 1,2,4-oxadiazoles,[49] and this may be the site of the metabolic fragility. Studies detailing the pharmacokinetics and localization of **6** to brain and spinal cord lesions in other EAE models are published elsewhere.[50]

Sodium channel blockade with **6** in vivo was found to be neuroprotective, preventing retinal ganglion cell loss in optic neuritis in this refined EAE model.[44] In this case, the mechanism of neuroprotection is unlikely to be due to peripheral immunosuppression that prevents disease from developing.[18,51] There was no evidence of T-cell immunosuppression seen here in a paradigm that can detect immunosuppressive doses of drugs even following a single dose. Furthermore, in our hands, overt immunosuppression does not affect the development of disease in conventional EAE using a similar delivery of sodium channel-blocking compounds including phenytoin, sipatrigine, carbamazepine, and oxcarbazepine,[50] which is in contrast to some studies where immunosuppression of sodium channel blockers delivered in the drinking water was noted.[18,51] This class of agents has consistently been found to be neuroprotective.[49] Neuroprotection with **6** is most likely to occur at the level of the axon or nerve and perhaps through inhibition of microglial
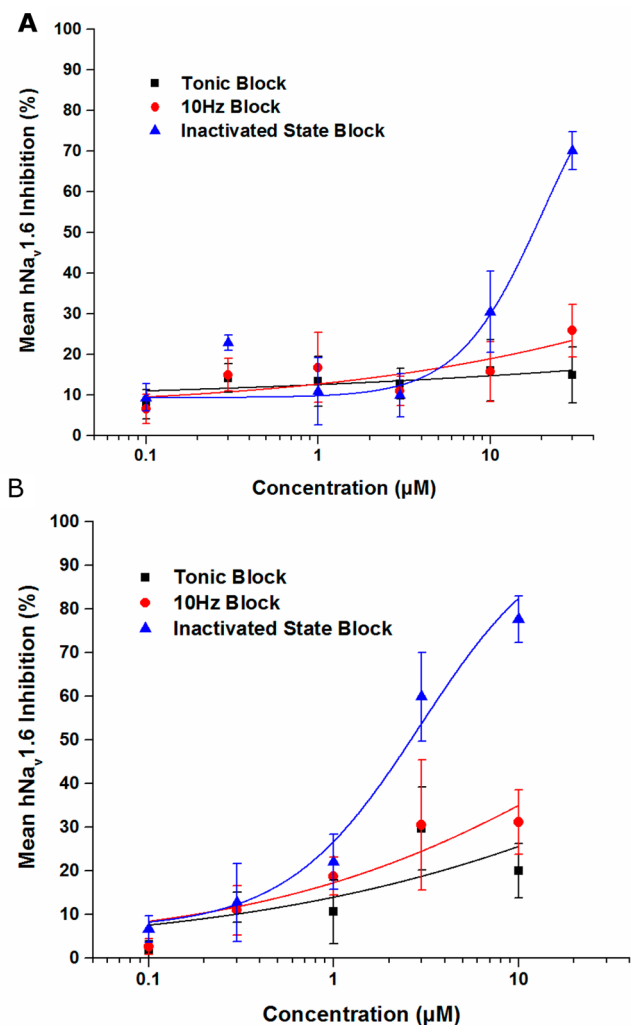
Figure 2. Detail of activity of **6** (A) and **51** (B) against the $Na_v1.6$ isoform. Blue triangles are block of the inactivated state, red circles are block of 10 Hz current, and black squares are block of tonic current.

Figure 3. T-cell immunosuppressive activity of **6** in vivo. Mice received epicutaneous application of 25 μL of 2.5% oxazolone (OX) in acetone olive oil (AOO) 4:1 on day 0 on the dorsum of the ear. Animals received daily intraperitoneal (i.p.) injections of either vehicle (DMSO/Cremophor/phosphate buffered saline, 1:1:18) or **6** from day −1 to day 2. On day 3, the draining auricular lymph nodes were removed from three mice and pooled, and a single-cell suspension was made. Lymph node cells were counted, and 5×10^5 cells per well, in triplicate, were cultured overnight at 37 °C. T-cell proliferation was assessed using the CellTiter 96 AQ_{ueous} Cell Proliferation Assay, which uses a MTS tetrazolium compound that is bioreduced by live cells. The resulting formazan product absorbance is recorded at 490 nM. The results represent the mean response ± SD of triplicate assays.

Figure 4. Retinal ganglion cells in the retina of mice (A) before or (B) after the development of optic neuritis. (C) Density of RGC. The box represents the 25th and 75th percentiles. The whiskers represent the fifth and 95th percentiles. The solid line represents the median. Differences between vehicle and drug-treated controls were assessed using Student's t test.

activity, which are probably central to the pathogenesis of progressive MS.[45,46]

Furthermore, some microglial responses are mediated via Na_v channel activity. Therefore, blockade of sodium channels could result in neuroprotective effects on immune and nonimmune components that may drive progressive nerve loss in MS.[45,46] Neurodegeneration accumulates slowly over time and therefore allows a larger time window for treatment onset compared to acute conditions such as stroke. Lesions in MS can develop throughout the neuroaxis but are common within the optic nerve, where optic neuritis is often an initial sign of disease. The visual pathway is the most accessible part of the human nervous system, and optic neuritis in MS is considered to be an ideal tissue to study the effect of neuroprotective treatments in MS and is being targeted in a number of studies.[47,48] Amiloride and phenytoin are currently in phase II clinical trials for the treatment of optic neuritis in MS (NCT01802489, NCT01451593).[48] We chose to utilize an optic neuritis model for in vivo evaluation of neuroprotection in this study.

Recently, lamotrigine was examined in progressive MS, but it did not appear to inhibit the development of brain atrophy, which was the primary outcome measure, although significant
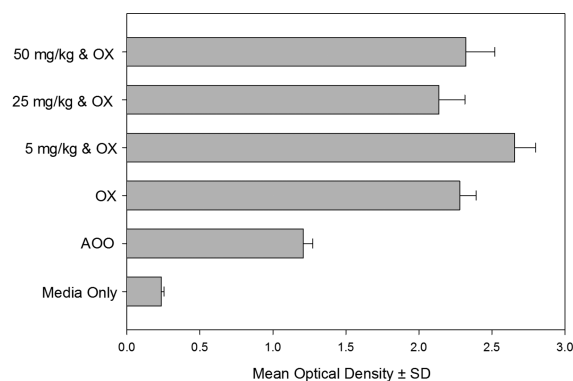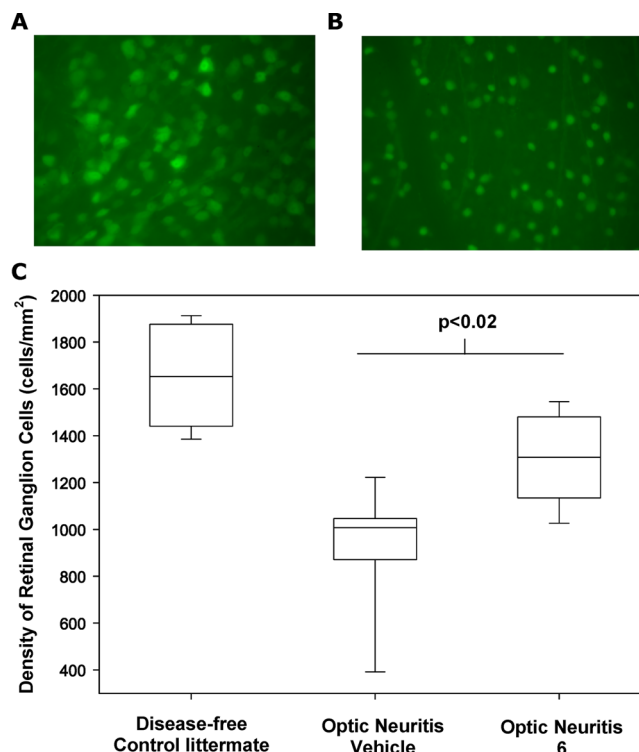
effects of slowing of walking deterioration were noted.[27] There is a clear need to evaluate better tolerated and more effective neuroprotective agents. The chemical series described here may

provide a platform for the development of pharmaceutical agents for the treatment of MS and other neurological diseases.

EXPERIMENTAL SECTION

All compounds were at least 95% pure as assayed by LCMS (electrospray positive). The preparations of analogues **6** and **51** are shown below, and the preparation of the remainder of the analogues is provided in the Supporting Information.

General Procedure for the Synthesis of Benzamide Analogues. To a solution of R-substituted benzoic acid (0.10 g, 0.82 mmol) in DMF (5 mL) were added HATU (0.34 g, 0.9 mmol, 1.1 equiv) and diisopropylethylamine (0.23 g, 0.31 mL, 1.8 mmol, 2.2 equiv), and the solution allowed to stir for half of an hour at room temperature under nitrogen. The amine (0.9 mmol, 1.1 equiv) was then added, and the brown solution was allowed to stir overnight. The DMF was removed in vacuo, and the resulting crude oil was dissolved in ethyl acetate and washed with water, 1 N HCl, 1 N NaHCO$_3$, and brine. The organic phase was then dried over magnesium sulfate, and the solvent was removed in vacuo. The crude oil was purified using flash chromatography, eluting with 10% methanol in dichloromethane.

General Procedure for the Synthesis of Sulfonamide N$_1$ Analogues. To a solution of the appropriate amine (0.22 g, 0.71 mmol, 1 equiv) in water (10 mL) was added R-substituted benzene sulfonyl chloride (0.78 mmol, 1.1 equiv). The solution was allowed to stir, and saturated sodium carbonate(aq) was added gradually to adjust the acidic pH to 8. The solution was then allowed to stir overnight at room temperature. The white precipitate was filtered off, washed with diethyl ether, and dried in vacuo.

***N*-[[5-[1-(2-Imidazol-1-ylethyl)indazol-3-yl]-1,2,4-oxadiazol-3-yl]methyl]benzamide (6).** Orange crystals (18% yield, 98% purity). ^{1}H NMR (300 MHz, DMSO) δ 9.27 (t, J = 5.7 Hz, 1H, NH), 8.13 (d, J = 8.1 Hz, 1H, ArH), 7.92 (d, J = 6.7 Hz, 2H, ArH), 7.64 (d, J = 8.5 Hz, 1H, ArH), 7.61−7.41 (m, 4H, ArH), 7.41−7.27 (m, 2H, ArH), 7.02 (s, 1H, ArH), 6.71 (s, 1H, ArH), 4.96 (t, J = 5.8 Hz, 2H, CH$_2$), 4.73 (d, J = 5.7 Hz, 2H, CH$_2$), 4.55 (t, J = 5.8 Hz, 2H, CH$_2$). ^{13}C NMR (75 MHz, CDCl$_3$) δ 170.1, 168.9, 166.5, 140.8, 137.2, 133.7, 131.5, 129.3, 128.4, 127.7, 127.4, 127.3, 123.7, 121.5, 120.3, 119.6, 110.5, 49.7, 45.7, 35.3. HRMS (TOF MS ES$^+$) calcd for C$_{22}$H$_{20}$N$_7$O$_2$ (MH$^+$), 414.1678; found, 414.1668.

***N*-[[5-[2-(2-Imidazol-1-ylethyl)indazol-3-yl]-1,2,4-oxadiazol-3-yl]methyl]-2-(trifluoromethoxy)benzamide (51).** ^{1}H NMR (300 MHz, CDCl$_3$) δ 8.18 (s, 1H, NH), 8.09 (d, J = 8.4 Hz, 1H, ArH), 7.99 (d, J = 7.7 Hz, 1H, ArH), 7.95 (s, 1H, ArH), 7.81 (d, J = 8.6 Hz, 1H, ArH), 7.54−7.30 (m, 5H, ArH), 6.69 (s, 1H, ArH), 6.30 (s, 1H, ArH), 5.37 (t, J = 5.5 Hz, 2H, CH$_2$), 4.82 (d, J = 5.1 Hz, 2H, CH$_2$), 4.55 (t, J = 5.5 Hz, 2H, CH$_2$). ^{13}C NMR (75 MHz, DMSO) δ 237.95, 168.13, 167.26, 164.96, 151.20, 148.34, 147.35, 137.33, 135.81, 130.68, 128.25, 127.08, 126.41, 125.70, 124.15, 122.28, 119.96, 119.79, 119.23, 118.23, 53.29, 45.60, 35.20. HRMS (TOF MS ES$^+$) calcd for C$_{25}$H$_{30}$N$_{10}$O$_5$ (MH$^+$), 498.1501; found, 498.1500.

In Vivo. *Animals.* Six to eight week old male and female wild-type and double-transgenic C57BL/6-Cg-Tg(Thy1-CFP)23Jrs.Tg (Tcra2D2,Tcrb2D2)1Kuch/J mice[44] were used from stock bred at Queen Mary University of London. Founder mice were originally obtained from Jackson Laboratories, Bar Habor, ME, USA). These transgenic mice express both a H-2A^b-restricted T-cell receptor (Vα3, Vβ11) specific for myelin oligodendrocyte glycoprotein residues 35−55 and a neuronally restricted Thy1 (CD90)-promoter-driven expression of cyan fluorescent protein, which is only present in the retinal ganglion cells within the retina.[44] Mice were maintained on a 12 h light/dark cycle with controlled humidity and temperature and housed as described previously.[52] The reporting of most aspects of the experimental design, which conform with the ARRIVE guidelines, has been described previously.[52] Animals were fed RM-1E diet and water ad libitum. All animal studies were approved by the Queen Mary ethical review panel and the United Kingdom Government Home Office Inspectorate. These studies conformed to the United Kingdom Animals (Scientific Procedures) Act 1986 for the use of animals in research.

In Vivo Local Lymph Node Assay. Mice (n = 3−4/group) received epicutaneous application of 25 μL of acetone/olive oil (4:1, AOO) or 25 μL of 2.5% oxazolone (OX, Sigma-Aldrich, Poole, UK) on day 0 on the dorsum of the ear. On day 3, the draining auricular lymph nodes were removed, and a single-cell suspension was made. Lymph node cells were counted, and 5×10^5 cells/well, in triplicate, were cultured overnight at 37 °C/5% CO$_2$ in 200 μL of RPMI-1640 medium supplemented with 10% heat-inactivated fetal calf serum, L-glutamine, sodium-pyruvate, and antibiotics as described previously.[42] T-cell proliferation was assessed using the CellTiter 96 AQ$_{ueous}$ Non-Radioactive Cell Proliferation Assay according to the manufacturer's instructions (Promega, Southhampton, UK). Animals received daily intraperitoneal (i.p.) injections of either DMSO/Cremophor/phosphate buffered saline (1:1:18) or **6** from day −1 to 2.

Optic Neuritis Multiple Sclerosis Mouse Model. Optic neuritis was induced in C57BL/6-Cg-Tg(Thy1-CFP)23Jrs.Tg(Tcra2D2, Tcrb2D2)1Kuch/J transgenic mice. Subclinical EAE in the absence of paralytical disease was induced following administration of 150 ng of *Bordetella pertussis* toxin (Sigma-Aldrich) in phosphate-buffered saline.[47] Optic neuritis within the optic nerve was augmented following the injection of 250 μg of Z12 rat IgG2b mouse myelin oligodendrocyte-specific demyelinating antibody on day 14.[47] Animals were injected daily from day 0−21 of the experiment with 5 mg/kg i.p. Animals were killed on day 21 postinduction, and eyes were enucleated and immersed in 4% paraformaldehyde (Sigma-Aldrich) in PBS (pH 7.4) overnight. The retinae were dissected, and the cornea, sclera, lens, hyaloid vasculature, and connective tissue were removed in 2× normal-strength PBS. Four radial incisions were cut around the retina, and flatmounts were mounted onto slides and coverslipped with antifade glycerol (CitiFluor Ltd., London, UK). The retinal flatmounts were imaged by fluorescent microscopy, retinal ganglion cell density was calculated by counting cyan fluorescent protein-expressing retinal ganglion cells using stereology software with a fractionator probe, and the number cells in the four quadrants around the optic nerve head was counted.[47] The parametric data was assessed using Student's t test, incorporating tests for equality of variance using SigmaStat software (Systat Software, Inc., San Jose, CA, USA).

ASSOCIATED CONTENT

⑤ Supporting Information

Additional biological methods and experimental details for synthesized compounds. This material is available free of charge via the Internet at http://pubs.acs.org.

AUTHOR INFORMATION

Corresponding Author

*Phone: +44 20 7679 2000. E-mail: d.selwood@ucl.ac.uk.

Notes

The authors declare no competing financial interest.

ACKNOWLEDGMENTS

ABBREVIATIONS USED

AOO, acetone olive oil; CNS, central nervous system; DIPEA, diisopropylethylamine; EAE, experimental autoimmune encephalomyelitis; HATU, *N*-[(dimethylamino)-1*H*-1,2,3-triazolo-[4,5-*b*]pyridin-1-ylmethylene]-*N*-methylmethanaminium hexafluorophosphate *N*-oxide; MS, multiple sclerosis; Na$_v$, voltage-gated sodium; OX, oxazolone; TCR, T-cell receptor

■ REFERENCES

(1) Tarnawa, I.; Bolcskei, H.; Kocsis, P. Blockers of voltage-gated sodium channels for the treatment of central nervous system diseases. *Recent Pat. CNS Drug Discovery* **2007**, *2*, 57−78.

(2) Mantegazza, M.; Curia, G.; Biagini, G.; Ragsdale, D. S.; Avoli, M. Voltage-gated sodium channels as therapeutic targets in epilepsy and other neurological disorders. *Lancet Neurol.* **2010**, *9*, 413−424.

(3) Choi, H.; Morrell, M. J. Review of lamotrigine and its clinical applications in epilepsy. *Expert Opin. Pharmacother.* **2003**, *4*, 243−251.

(4) Ambrosio, A. F.; Soares-Da-Silva, P.; Carvalho, C. M.; Carvalho, A. P. Mechanisms of action of carbamazepine and its derivatives, oxcarbazepine, BIA 2-093, and BIA 2-024. *Neurochem. Res.* **2002**, *27*, 121−130.

(5) Errington, A. C.; Stohr, T.; Heers, C.; Lees, G. The investigational anticonvulsant lacosamide selectively enhances slow inactivation of voltage-gated sodium channels. *Mol. Pharmacol.* **2008**, *73*, 157−169.

(6) Catterall, W. A. Voltage-gated sodium channels at 60: Structure, function and pathophysiology. *J. Physiol.* **2012**, *590*, 2577−2589.

(7) Payandeh, J.; Gamal El-Din, T. M.; Scheuer, T.; Zheng, N.; Catterall, W. A. Crystal structure of a voltage-gated sodium channel in two potentially inactivated states. *Nature* **2012**, *486*, 135−139.

(8) Payandeh, J.; Scheuer, T.; Zheng, N.; Catterall, W. A. The crystal structure of a voltage-gated sodium channel. *Nature* **2011**, *475*, 353−358.

(9) Ulbricht, W. Sodium channel inactivation: Molecular determinants and modulation. *Physiol. Rev.* **2005**, *85*, 1271−1301.

(10) Lai, J.; Hunter, J. C.; Porreca, F. The role of voltage-gated sodium channels in neuropathic pain. *Curr. Opin. Neurobiol.* **2003**, *13*, 291−297.

(11) Wood, J. N.; Boorman, J. Voltage-gated sodium channel blockers; target validation and therapeutic potential. *Curr. Top. Med. Chem.* **2005**, *5*, 529−537.

(12) Costigan, M.; Scholz, J.; Woolf, C. J. Neuropathic pain: A maladaptive response of the nervous system to damage. *Annu. Rev. Neurosci.* **2009**, *32*, 1−32.

(13) Dib-Hajj, S. D.; Black, J. A.; Waxman, S. G. Voltage-gated sodium channels: Therapeutic targets for pain. *Pain Med.* **2009**, *10*, 1260−1269.

(14) Theile, J. W.; Cummins, T. R. Recent developments regarding voltage-gated sodium channel blockers for the treatment of inherited and acquired neuropathic pain syndromes. *Front. Pharmacol.* **2011**, *2*, 54.

(15) Zuliani, V.; Rivara, M.; Fantini, M.; Costantino, G. Sodium channel blockers for neuropathic pain. *Expert Opin. Ther. Pat.* **2010**, *20*, 755−779.

(16) Hoyt, S. B.; London, C.; Gorin, D.; Wyvratt, M. J.; Fisher, M. H.; Abbadie, C.; Felix, J. P.; Garcia, M. L.; Li, X.; Lyons, K. A.; McGowan, E.; MacIntyre, D. E.; Martin, W. J.; Priest, B. T.; Ritter, A.; Smith, M. M.; Warren, V. A.; Williams, B. S.; Kaczorowski, G. J.; Parsons, W. H. Discovery of a novel class of benzazepinone $Na_v1.7$ blockers: Potential treatments for neuropathic pain. *Bioorg. Med. Chem. Lett.* **2007**, *17*, 4630−4634.

(17) Hoyt, S. B.; London, C.; Abbadie, C.; Felix, J. P.; Garcia, M. L.; Jochnowitz, N.; Karanam, B. V.; Li, X.; Lyons, K. A.; McGowan, E.; Priest, B. T.; Smith, M. M.; Warren, V. A.; Thomas-Fowlkes, B. S.; Kaczorowski, G. J.; Duffy, J. L. A novel benzazepinone sodium channel blocker with oral efficacy in a rat model of neuropathic pain. *Bioorg. Med. Chem. Lett.* **2013**, *23*, 3640−3645.

(18) Waxman, S. G. Mechanisms of disease: Sodium channels and neuroprotection in multiple sclerosis-current status. *Nat. Clin. Pract. Neurol.* **2008**, *4*, 159−169.

(19) Mongin, A. A. Disruption of ionic and cell volume homeostasis in cerebral ischemia: The perfect storm. *Pathophysiology* **2007**, *14*, 183−193.

(20) Stankowski, J. N.; Gupta, R. Therapeutic targets for neuroprotection in acute ischemic stroke: Lost in translation? *Antioxid. Redox Signaling* **2011**, *14*, 1841−1851.

(21) Crumrine, R. C.; Bergstrand, K.; Cooper, A. T.; Faison, W. L.; Cooper, B. R. Lamotrigine protects hippocampal CA1 neurons from ischemic damage after cardiac arrest. *Stroke* **1997**, *28*, 2230−2236.

(22) Fujitani, T.; Adachi, N.; Miyazaki, H.; Liu, K.; Nakamura, Y.; Kataoka, K.; Arai, T. Lidocaine protects hippocampal neurons against ischemic damage by preventing increase of extracellular excitatory amino acids: A microdialysis study in Mongolian gerbils. *Neurosci. Lett.* **1994**, *179*, 91−94.

(23) Graham, S. H.; Chen, J.; Lan, J.; Leach, M. J.; Simon, R. P. Neuroprotective effects of a use-dependent blocker of voltage-dependent sodium channels, BW619C89, in rat middle cerebral artery occlusion. *J. Pharmacol. Exp. Ther.* **1994**, *269*, 854−859.

(24) Lekieffre, D.; Meldrum, B. S. The pyrimidine-derivative, BW1003C87, protects CA1 and striatal neurons following transient severe forebrain ischaemia in rats. A microdialysis and histological study. *Neuroscience* **1993**, *56*, 93−99.

(25) Cheng, Y. D.; Al-Khoury, L.; Zivin, J. A. Neuroprotection for ischemic stroke: Two decades of success and failure. *NeuroRx* **2004**, *1*, 36−45.

(26) Onteniente, B.; Rasika, S.; Benchoua, A.; Guegan, C. Molecular pathways in cerebral ischemia: Cues to novel therapeutic strategies. *Mol. Neurobiol.* **2003**, *27*, 33−72.

(27) Kapoor, R.; Furby, J.; Hayton, T.; Smith, K. J.; Altmann, D. R.; Brenner, R.; Chataway, J.; Hughes, R. A.; Miller, D. H. Lamotrigine for neuroprotection in secondary progressive multiple sclerosis: A randomised, double-blind, placebo-controlled, parallel-group trial. *Lancet Neurol.* **2010**, *9*, 681−688.

(28) Van der Walt, A.; Butzkueven, H.; Kolbe, S.; Marriott, M.; Alexandrou, E.; Gresle, M.; Egan, G.; Kilpatrick, T. Neuroprotection in multiple sclerosis: A therapeutic challenge for the next decade. *Pharmacol. Ther.* **2010**, *126*, 82−93.

(29) Yu, F. H.; Catterall, W. A. Overview of the voltage-gated sodium channel family. *Genome Biol.* **2003**, *4*, 207.

(30) Whitaker, W. R.; Faull, R. L.; Waldvogel, H. J.; Plumpton, C. J.; Emson, P. C.; Clare, J. J. Comparative distribution of voltage-gated sodium channel proteins in human brain. *Brain Res.* **2001**, *88*, 37−53.

(31) Kaplan, M. R.; Cho, M. H.; Ullian, E. M.; Isom, L. L.; Levinson, S. R.; Barres, B. A. Differential control of clustering of the sodium channels Na(v)1.2 and Na(v)1.6 at developing CNS nodes of Ranvier. *Neuron* **2001**, *30*, 105−119.

(32) Mao, Q.; Jia, F.; Zhang, X. H.; Qiu, Y. M.; Ge, J. W.; Bao, W. J.; Luo, Q. Z.; Jiang, J. Y. The up-regulation of voltage-gated sodium channel Nav1.6 expression following fluid percussion traumatic brain injury in rats. *Neurosurgery* **2010**, *66*, 1134−1139.

(33) Waxman, S. G. Axonal conduction and injury in multiple sclerosis: The role of sodium channels. *Nat. Rev. Neurosci.* **2006**, *7*, 932−941.

(34) Yuen, T. J.; Browne, K. D.; Iwata, A.; Smith, D. H. Sodium channelopathy induced by mild axonal trauma worsens outcome after a repeat injury. *J. Neurosci. Res.* **2009**, *87*, 3620−3625.

(35) Wang, J. A.; Lin, W.; Morris, T.; Banderali, U.; Juranka, P. F.; Morris, C. E. Membrane trauma and Na^+ leak from Nav1.6 channels. *Am. J. Physiol.: Cell Physiol.* **2009**, *297*, C823−C834.

(36) Boucher, P. A.; Joos, B.; Morris, C. E. Coupled left-shift of Nav channels: Modeling the Na^+-loading and dysfunctional excitability of damaged axons. *J. Comput. Neurosci.* **2012**, *33*, 301−319.

(37) Yao, C.; Williams, A. J.; Cui, P.; Berti, R.; Hunter, J. C.; Tortella, F. C.; Dave, J. R. Differential pattern of expression of voltage-gated sodium channel genes following ischemic brain injury in rats. *Neurotoxic. Res.* **2002**, *4*, 67−75.

(38) Huang, X. J.; Mao, Q.; Lin, Y.; Feng, J. F.; Jiang, J. Y. Expression of voltage-gated sodium channel Nav1.3 is associated with severity of traumatic brain injury in adult rats. *J. Neurotrauma* **2013**, *30*, 39−46.

(39) Clutterbuck, L. A.; Posada, C. G.; Visintin, C.; Riddall, D. R.; Lancaster, B.; Gane, P. J.; Garthwaite, J.; Selwood, D. L. Oxadiazolylindazole sodium channel modulators are neuroprotective toward hippocampal neurones. *J. Med. Chem.* **2009**, *52*, 2694−2707.

(40) Fowler, J. C.; Li, Y. Contributions of Na^+ flux and the anoxic depolarization to adenosine 5′-triphosphate levels in hypoxic/hypoglycemic rat hippocampal slices. *Neuroscience* **1998**, *83*, 717−722.

(41) Watson, C. M.; Davison, A. N.; Baker, D.; O'Neill, J. K.; Turk, J. L. Suppression of demyelination by mitoxantrone. *Int. J. Immunopharmacol.* **1991**, *13*, 923−930.

(42) O'Neill, J. K.; Baker, D.; Davison, A. N.; Maggon, K. K.; Jaffee, B. D.; Turk, J. L. Therapy of chronic relapsing experimental allergic encephalomyelitis and the role of the blood-brain barrier: Elucidation by the action of Brequinar sodium. *J. Neuroimmunol.* **1992**, *38*, 53−62.

(43) Baker, D.; O'Neill, J. K.; Davison, A. N.; Turk, J. L. Control of immune-mediated disease of the central nervous system requires the use of a neuroactive agent: Elucidation by the action of mitoxantrone. *Clin. Exp. Immunol.* **1992**, *90*, 124−128.

(44) Lidster, K.; Jackson, S. J.; Ahmed, Z.; Munro, P.; Coffey, P.; Giovannoni, G.; Baker, M. D.; Baker, D. Neuroprotection in a novel mouse model of multiple sclerosis. *PLoS One* **2013**, *8*, e79188-1−e79188-15.

(45) Black, J. A.; Waxman, S. G. Sodium channels and microglial function. *Exp. Neurol.* **2012**, *234*, 302−315.

(46) Morsali, D.; Bechtold, D.; Lee, W.; Chauhdry, S.; Palchaudhuri, U.; Hassoon, P.; Snell, D. M.; Malpass, K.; Piers, T.; Pocock, J.; Roach, A.; Smith, K. J. Safinamide and flecainide protect axons and reduce microglial activation in models of multiple sclerosis. *Brain* **2013**, *136*, 1067−1082.

(47) Lidster, K.; Baker, D. Optical coherence tomography detection of neurodegeneration in multiple sclerosis. *CNS Neurol. Disord.: Drug Targets* **2012**, *11*, 518−527.

(48) Raftopoulos, R. E.; Kapoor, R. Neuroprotection for acute optic neuritis—Can it work? *Mult. Scler. Relat. Disord.* **2013**, *2*, 307−311.

(49) Bostrom, J.; Hogner, A.; Llinas, A.; Wellner, E.; Plowright, A. T. Oxadiazoles in medicinal chemistry. *J. Med. Chem.* **2012**, *55*, 1817−1830.

(50) Al-Izki, S.; Pryce, G.; Hankey, D. J.; Lidster, K.; von Kutzleben, S. M.; Browne, L.; Clutterbuck, L.; Posada, C.; Edith Chan, A. W.; Amor, S.; Perkins, V.; Gerritsen, W. H.; Ummenthum, K.; Peferoen-Baert, R.; van der Valk, P.; Montoya, A.; Joel, S. P.; Garthwaite, J.; Giovannoni, G.; Selwood, D. L.; Baker, D. Lesional-targeting of neuroprotection to the inflammatory penumbra in experimental multiple sclerosis. *Brain* **2013**, *137*, 92−98.

(51) Black, J. A.; Liu, S.; Hains, B. C.; Saab, C. Y.; Waxman, S. G. Long-term protection of central axons with phenytoin in monophasic and chronic-relapsing EAE. *Brain* **2006**, *129*, 3196−3208.

(52) Al-Izki, S.; Pryce, G.; O'Neill, J. K.; Butter, C.; Giovannoni, G.; Amor, S.; Baker, D. Practical guide to the induction of relapsing progressive experimental autoimmune encephalomyelitis in the Biozzi ABH mouse. *Mult. Scler. Relat. Disord.* **2012**, *1*, 29−38.